Journal of Structural Geology, Vol. 10, No. 3, pp. 283 to 296, 1988
Printed in Great Britain

0191-8141/88 $03.00 + 0.00

Fluid flow, metasomatism and amphibole deformation in an imbricated ophiolite, North Cascades, Washington

R. B. MILLER

Department of Geology, San Jose State University, San Jose, CA 95192, U.S.A.

(*Received* 11 *February* 1987; *accepted in revised form* 3 *December* 1987)

Abstract—Metasomatic tremolite-rich mylonites are widespread in imbricate thrust slices of ultramafic rocks of the ophiolitic Ingalls Complex in Washington State. Protoliths for these amphibolite-facies mylonites were peridotite and serpentinite. Abundant syntectonic tremolite veins in the ultramafites record narrowly channelized flow of infiltrating fluids, whereas metasomatic mylonite zones record more pervasive flow. Fluids were probably released mainly by prograde devolatization reactions within serpentinite and mafic ophiolitic rocks that experienced earlier hydrothermal metamorphism.

Olivine apparently deformed by dislocation creep in the mylonites. In the tremolite-rich rocks, locally preserved amphibole porphyroclasts deformed mainly by microfracturing. Acicular tremolites, which dominate the mylonites, form syntectonic overgrowths on porphyroclasts and probably record diffusive mass transfer which may have accompanied cataclasis. Acicular tremolites subsequently were folded and define both post-crystalline crenulations and polygonal arcs.

Fluid flow, deformation and metamorphism were apparently complexly interrelated in the imbricate zone. Thrusts juxtaposed contrasting rock types that were sources and sinks for fluids, and shear zones focused fluid flow. Metamorphism probably facilitated deformation through the release of fluids during dehydration reactions. High fluid pressure may have led to hydraulic fracturing and may have controlled strain softening in the tremolitic mylonite zones as it favored microcracking and diffusive mass transfer over dislocation creep. Infiltrating metasomatic fluids probably play an important role in the evolution of shear zones in many ultramafic bodies during medium-grade metamorphism.

INTRODUCTION

FLUIDS and metamorphic reactions can strongly influence the mechanical properties of rocks during deformation in fault zones. Chemical changes clearly accompany deformation within some small-scale shear zones (e.g. Beach 1976, 1980, Kerrich *et al.* 1977, Brodie 1980, Borges & White 1980, Sinha *et al.* 1986). However, less is known about the relationships between metasomatic fluids and deformation within thick, syn-metamorphic imbricate thrust zones (e.g. Jamieson & Strong 1981).

In this paper, the interaction of fluid transport, metamorphism and deformation during imbricate thrusting of an ophiolite, the Ingalls Complex of Washington State, is described. I intend to show that deformation and metamorphism of ultramafic rocks of this ophiolite were influenced by infiltration of metasomatic fluids along shear zones and other structural channels. This focused fluid flow resulted in the formation of amphibole-rich metasomatic rocks that comprise most of the mylonites formed during thrusting.

FIELD RELATIONS

The well-exposed Ingalls Complex is a large (400 km^2), disrupted late Jurassic ophiolite dominated by 'mantle-type' ultramafic tectonites. The ophiolite was emplaced onto the crystalline core of the North Cascades by the Windy Pass Thrust (Miller 1980, 1985) which is exposed in a 75 km^2 roof pendant on the late Cretaceous Mount Stuart Batholith (Fig. 1). The pelitic Chiwaukum Schist of the crystalline core makes up the lower plate of the thrust. In the upper plate, the Ingalls is imbricated both internally and with a group of orthogneisses, amphibolites, biotite schists and quartzitic schists (Heterogeneous Metamorphic Suite) that are lithologically distinct from the Chiwaukum Schist (Miller 1985) (Figs. 1 and 2). Imbrication probably coincided with amphibolite-facies metamorphism of the ophiolite, but final movement on the sole thrust postdated metamorphism of both the lower and upper plates and carried the imbricate slices northwards onto the Chiwaukum Schist.

Thrusting apparently occurred in the mid-Cretaceous. One orthogneiss in a slice of the Heterogeneous Metamorphic Suite has yielded a preliminary U–Pb zircon age of 96 Ma (Hoppe, in Miller 1985) and the 87–93 Ma Mount Stuart Batholith (Engels & Crowder 1971) sharply truncates the imbricate thrusts and the Windy Pass Thrust (Figs. 1 and 2). The batholith is essentially undeformed in the map area, showing only a weak foliation in its margins.

The amphibolite-facies metamorphism of basal ultramafites in the Ingalls contrasts with many ophiolites which are characterized by basal zones of serpentinite mélange or very high-grade mylonitic peridotite (e.g. Nicolas *et al.* 1980). The tectonic setting and source of heat for the syn-imbrication metamorphism of the ophiolite are unclear. The metamorphism is absent in the structurally higher portion of the Ingalls to the south (Fig. 1), and appears to be related to thrusting, but lacks the steep thermal gradients (Miller 1980) recorded by dynamothermal aureoles at the bases of some ophiolites

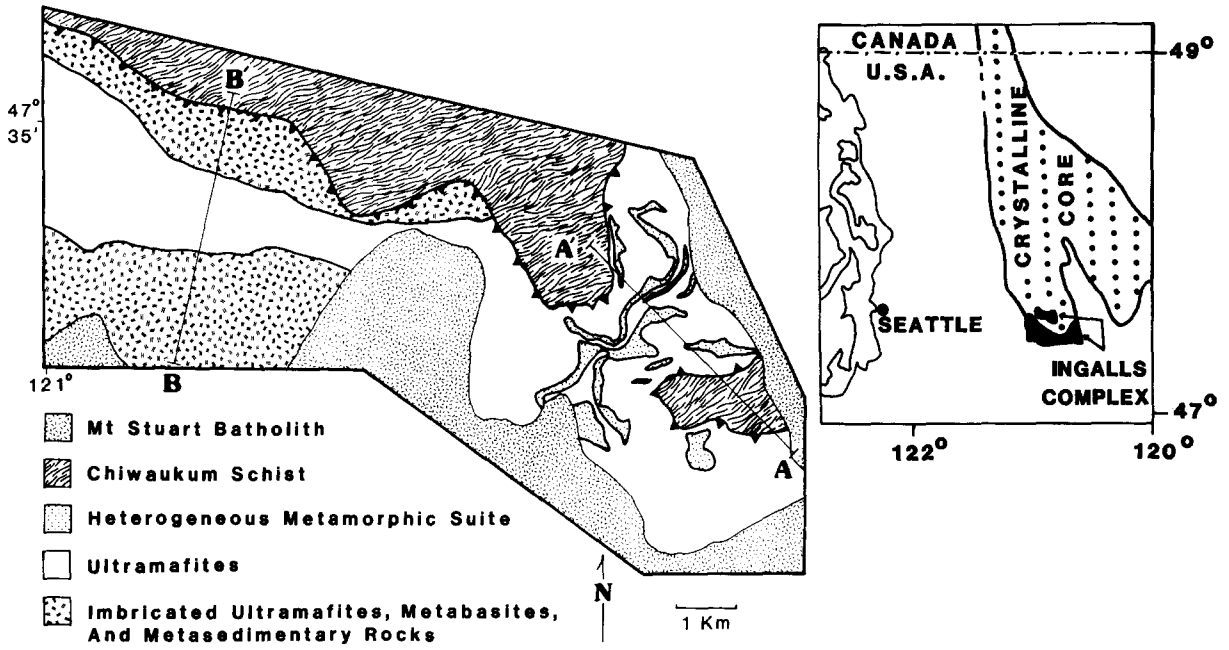

Fig. 1. Simplified geological map of the roof pendant of the Mt Stuart Batholith. See Miller (1985) for a more detailed version. All faults are thrusts, but 'teeth' are shown only for the Windy Pass Thrust. Inset shows the location of the Ingalls Complex and the position of the roof pendant relative to a larger, structurally higher outcrop belt of the complex to the south which escaped the amphibolite-facies event.

(e.g. Williams & Smyth 1973, Malpas 1979, Ghent & Stout 1981). The metamorphism may have resulted from shear heating during thrusting or, more likely, the regional thermal high associated with metamorphism and plutonism in the crystalline core of the North Cascades. A residual heat source for the ultramafites is unlikely as imbrication probably occurred about 60 Ma after generation of the ophiolite (Miller 1985).

Amphibolite-facies mylonites were formed from a variety of rock types during imbrication, but ultramafic mylonites are by far the most voluminous. Deformation was heterogeneously distributed within the ultramafic slices. Many of the thinner (<20 m thick) slices are pervasively mylonitized and almost all of the slices have mylonitic margins (Fig. 3a). Mylonites also occur in the interiors of thicker ultramafic slices; some occur as sharply bounded ductile shear zones, while others grade into less well-foliated, coarser-grained rocks.

The mylonitic foliation (S_m) cuts mantle-type structures (S_0 and S_1; Table 1) preserved in parts of thicker ultramafic slices (Fig. 3a). A mineral lineation (L_m, L_2) and a later lineation marked by crenulation axes (L_3) occur in many of the mylonites. The mylonite zones are commonly parallel to imbricate thrusts, but are truncated by the sole thrust in the eastern portion of the imbricate zone (Figs. 2 and 3).

Deformation was concentrated in, although not restricted to, metasomatic rocks, as ultramafites in both marginal and internal mylonite zones generally contain much more tremolite and chlorite than less-deformed metaperidotites. Nearly monomineralic layers of tremolite and chlorite typify the marginal zones and a pronounced banding is developed where these layers alternate with mylonitic, olivine-rich metaperidotite (Fig. 4a). Banded zones commonly extend for several meters from contacts of ultramafic slices. Tremolitic layers are more abundant than chloritic bands, particularly as the distance from contacts increases.

Tremolitic layers and less common chloritic bands also occur in many of the internal shear zones where they

Table 1. Fabric elements in the ultramafic rocks

Fabric element	Description	Interpretation
S_0	Defined by alternating olivine- and pyroxene-rich layers and their later metamorphic products	Metamorphic-differentiation layering formed in mantle
S_1	Defined by elongate spinel aggregates and pyroxene. Locally, axial-planar to isoclinal folds of transposed S_0	Flattening foliation formed in mantle
S_2, S_m	Defined mainly by aligned tremolite, compositional layering and grain-size layering (see text)	Formed during thrust emplacement of Ingalls; synchronous with amphibolite-facies metamorphism
L_2, L_m	Defined by amphiboles, mineral aggregates and fold axes, F_2	Synchronous with S_2
S_3	Defined by discrete zones of orientated tremolite; approximately axial-planar to small folds; anastomosing and spaced	Formed during thrust emplacement of Ingalls
L_3	Defined by axes of small folds, F_3	Synchronous with S_3

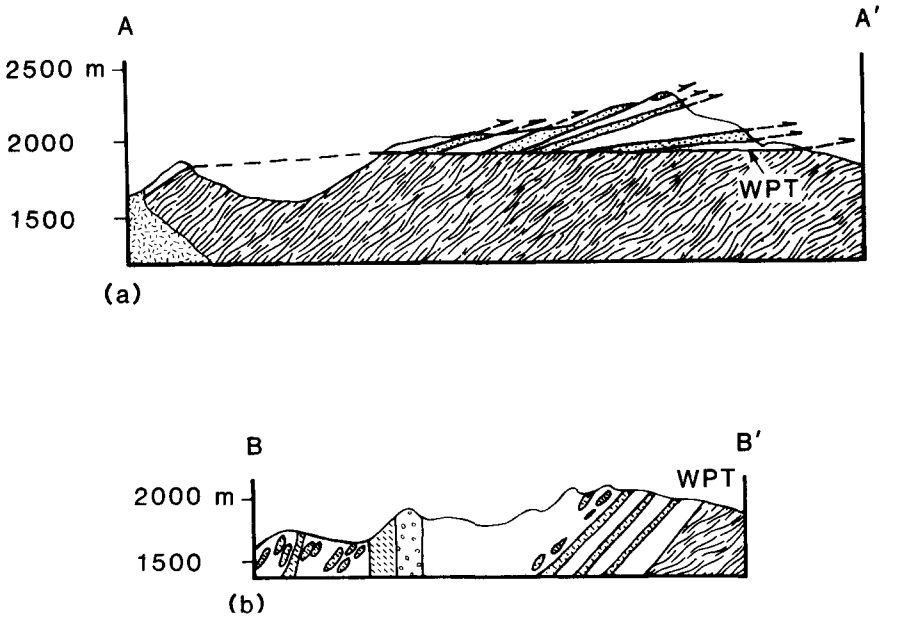

Fig. 2. (a) Cross-section through the eastern portion of the imbricate zone. WPT—Windy Pass Thrust. Other symbols are identical to those in Fig. 1. (b) Cross-section through the western portion of the imbricate zone. Section shows somewhat schematically only a few of the numerous fault slices in the area mapped in Fig. 1 as 'imbricated ultramafites, metabasites and metasedimentary rocks'. Dashed pattern—metabasite slices; open circles—metasedimentary rocks of the Ingalls Complex; other symbols are identical to those in Fig. 1. Note the steepening of fault slices relative to the eastern part of the imbricate zone, the relatively pod-like shapes of slices, and the sub-parallelism of the fault slices and the Windy Pass Thrust. In both cross-sections, more detail is shown than is displayed in Fig. 1.

range up to 1 m in thickness. Numerous layers are present in some internal shear zones, imparting a strongly banded appearance, but single layers of tremolite occur in other zones. In addition, a centimeter-scale gneissic layering defined by discontinuous forsterite- and tremolite-rich bands occurs in many internal zones.

Mylonitization may have occurred in part during formation of the monomineralic layers in both marginal and internal mylonitic zones (see below). Subsequent deformation is recorded by strongly boudinaged layers (Fig. 4b) and locally chaotic crenulations of the mylonitic foliation in tremolite-rich rocks. Narrow, discontinuous zones of weakly foliated, retrograde serpentinite also occur locally and postdate all other structures.

Syntectonic veins of tremolite and less commonly of talc riddle the ultramafic slices, but do not form a network. Veins are particularly abundant near mylonite zones. The tremolite veins can be subdivided into several types (Fig. 3b): early veins subparallel (<25°) to S_m; late veins subnormal to S_m; and subordinate late conjugate veins oriented at about 60° to S_m. The identical mineralogy in the various types suggests that they formed during the same metamorphic event.

The tremolite veins show variable degrees of deformation. The earliest subparallel veins typically have been flattened and/or swirled. Tremolite fibers are commonly oriented at angles of 20° to vein walls, and folds of fibers occur within some of the more strongly deformed veins. Tremolite has been completely recrystallized in still other subparallel veins. In many places, it is difficult to distinguish deformed veins from S_m compositional layers, and some (many?) tremolitic bands in gneissic, mylonitic metaperidotites may be veins that have been progressively rotated and flattened into S_m. In contrast, subnormal veins generally are only weakly deformed or undeformed and typically cut S_m and the subparallel veins.

METAMORPHIC ASSEMBLAGES AND *P–T* CONDITIONS

The ultramafites consist mainly of forsterite, clinoamphibole and chlorite, with lesser talc and enstatite. All clinoamphiboles are identified as tremolite by standard petrographic techniques, although the variety of amphibole textures (see below) conceivably reflects some compositional differences. The ultramafites have been subdivided into three types on the basis of the modal percentages of the major phases:

Type 1: forsterite >70%, tremolite + chlorite <25%;

Type 2: forsterite 20–65%, tremolite + chlorite 35–80%;

Type 3: tremolite + chlorite >80%, forsterite absent.

The three types grade into one another, and reflect differences in the amount of metasomatic transformation. This division is also structurally significant. Type 1 rocks make up most of the non-mylonitic ultramafites and occur in some mylonite zones. Type 2 ultramafites characterize internal zones, but also occur in marginal mylonite zones, whereas type 3 ultramafites dominate marginal zones and are less common in internal mylonite zones. In general, tremolite-rich type 3 ultramafites (tremolitites) are the most strongly foliated rocks in the imbricate zone.

Mineralogic evidence of 'mantle-type' metamorphism is only preserved in the type 1 ultramafites which locally

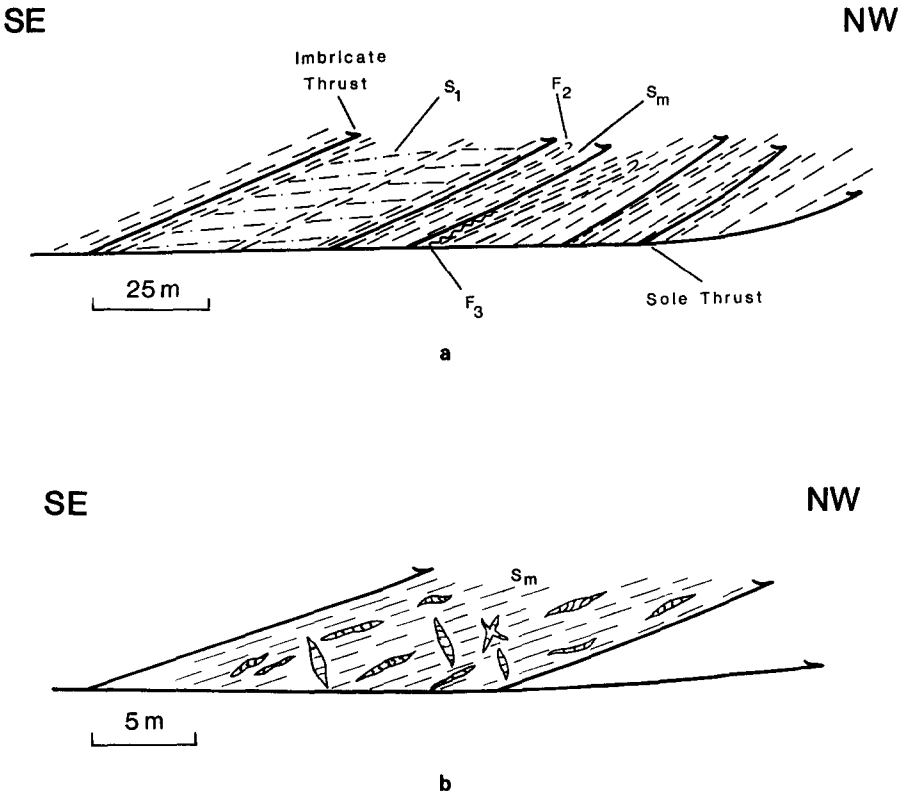

Fig. 3. (a) Diagrammatic sketch of relationships among imbricate thrusts, sole thrust, mylonitic foliation (S_m), mantle fabric (S_1), intrafolial F_2 folds, and F_3 crenulations in the eastern part of the imbricate zone. The spacing of dashed lines reflects the intensity of S_m. Note the angular discordance between S_m and the mantle fabric (S_1) preserved in a thick ultramafic slice. The size of F_2 and F_3 folds is exaggerated. (b) Diagrammatic sketch of an ultramafic slice showing the relationships among S_m, deformed sub-parallel tremolite veins, less deformed, generally thicker, sub-normal veins, and rare conjugate veins. Lines within the veins show the orientation of tremolite fibers. Vein thicknesses range from 0.5 to 15 cm, and are exaggerated in this figure.

contain the relict assemblage forsterite–enstatite–chrome spinel. The dominant equilibrium assemblage in the type 1 ultramafites is forsterite–tremolite–talc–chlorite, indicating crustal metamorphism in the middle amphibolite facies (Trommsdorff & Evans 1974). Somewhat higher temperatures (sillimanite zone) are indicated by the occurrence of forsterite–enstatite ± tremolite ± chlorite in some type 1 rocks. This enstatite shows distinctly different textures than the enstatite in the 'mantle-type' rocks (see below). Retrograde serpentine has replaced olivine in minor amounts in many samples.

The type 2 ultramafites generally contain forsterite–tremolite–chlorite. Forsterite–tremolite–Al spinel was recognized in one mylonite. The dominant assemblage in the type 3 ultramafites is tremolite–chlorite. This high-variance assemblage is relatively insensitive to pressure (P) and temperature (T), and may record conditions ranging from greenschist to upper amphibolite facies (Evans 1982).

It is difficult to establish whether presumed equilibrium assemblages in the three types of ultramafites formed contemporaneously. The assemblages are broadly compatible, and the three types show parallel fabrics, suggesting recrystallization during a single, although possibly protracted, event. Alternatively, S_m may be a composite fabric, and the assemblages defining S_m may not all be of the same generation. In this interpretation, the coincidence of orientations of S_m, and their parallelism with imbricate thrusts, reflect rotation of earlier fabrics into alignment with the thrusts.

Nevertheless, the assemblages probably constrain temperatures for at least the latest recrystallization of the ultramafites. The absence of serpentine, except as a static retrograde phase, provides a minimum T of 450–500°C for type 1 and type 2 ultramafites (Evans *et al.* 1976). The upper stability limit of forsterite–talc is about 675°C (Chernosky 1976), thereby limiting temperatures for the dominant assemblage in the type 1 rocks. However, the assemblage of forsterite–enstatite–tremolite–chlorite is stable to about 750°C (at 500 MPa), the breakdown temperature of chlorite (Zen 1972). This minor assemblage suggests that initial(?) deformation in the imbricate zone may have occurred at higher temperatures than those recorded by the dominant assemblages in the type 1 and type 2 ultramafites.

The lower temperature limit recorded by the type 2 ultramafic rocks is also 450–500°C, but the upper limit is less tightly constrained. Chlorite occurs in most type 2 rocks, again indicating a maximum T of about 750°C (assuming 500 MPa). The only limit that can be placed on the type 3 rocks is that temperatures were also less than that for chlorite breakdown.

The various assemblages are essentially insensitive to pressure, but a minimum of 150 MPa is inferred from the

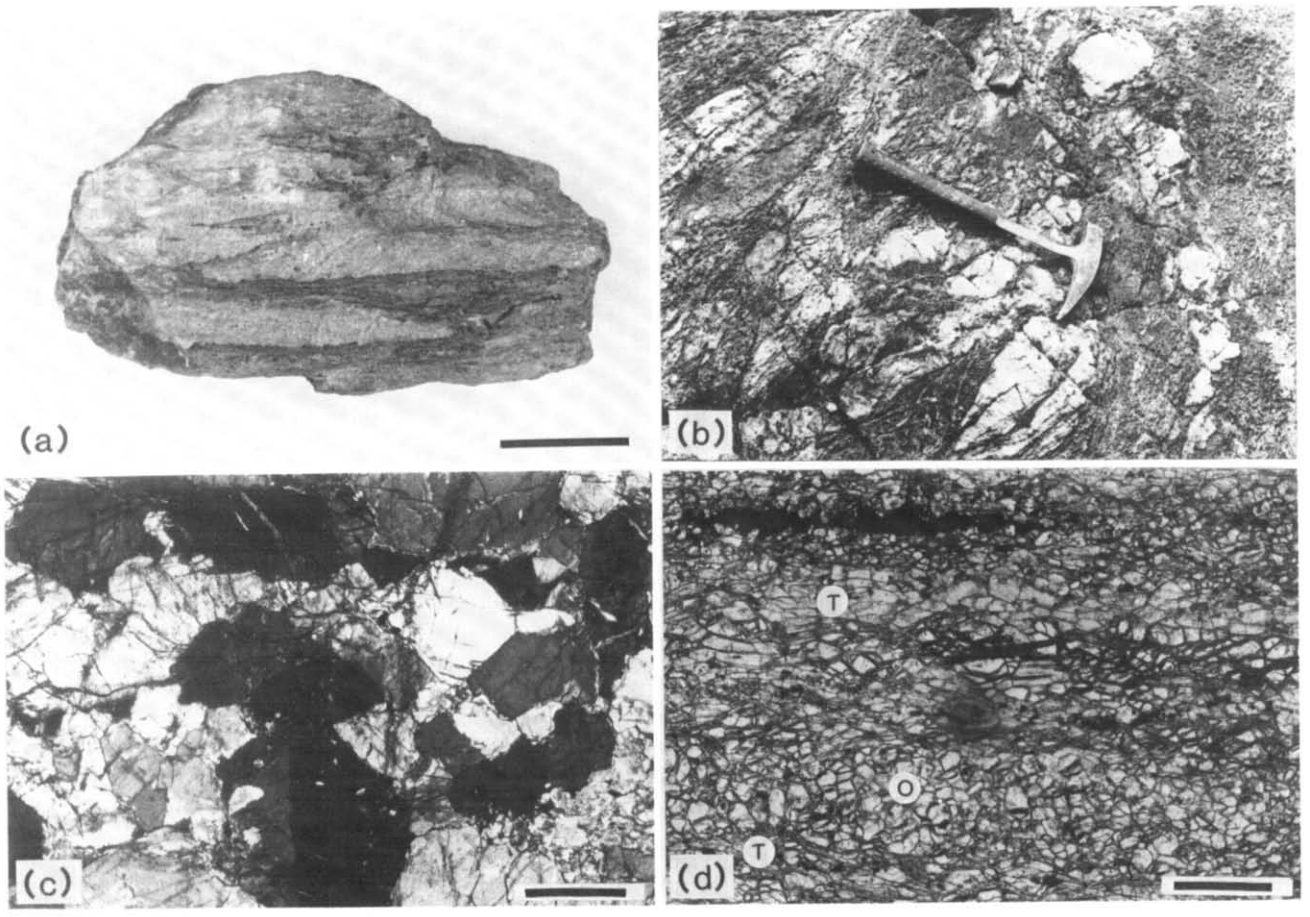

Fig. 4. (a) Sample of a metasomatic peridotite displaying bands of monomineralic tremolite (white) and of olivine-rich (thin-ribbed) ultramafite. The tremolite bands may be strongly deformed veins. Scale bar is 3 cm. (b) Boudinaged bands (white) of amphibole-rich mylonitic type 3 ultramafite (tremolitite) in metaperidotite in an internal mylonite zone. (c) Weakly porphyroclastic (relict mantle) texture in an olivine-rich type 1 ultramafite. Note the kinked olivine in the lower center of the figure. Scale bar is 0.5 mm. (d) Equilibrium textures in a well-recrystallized type 2 ultramafite. Bands of olivine (O) alternate with layers of tabular tremolite (T). It is not clear whether this clinoamphibole is identical compositionally to the fibrous tremolite in Fig. 5(b)–(e). This sample conceivably records a deformation prior to growth and deformation of acicular tremolite. Scale bar is 0.5 mm.

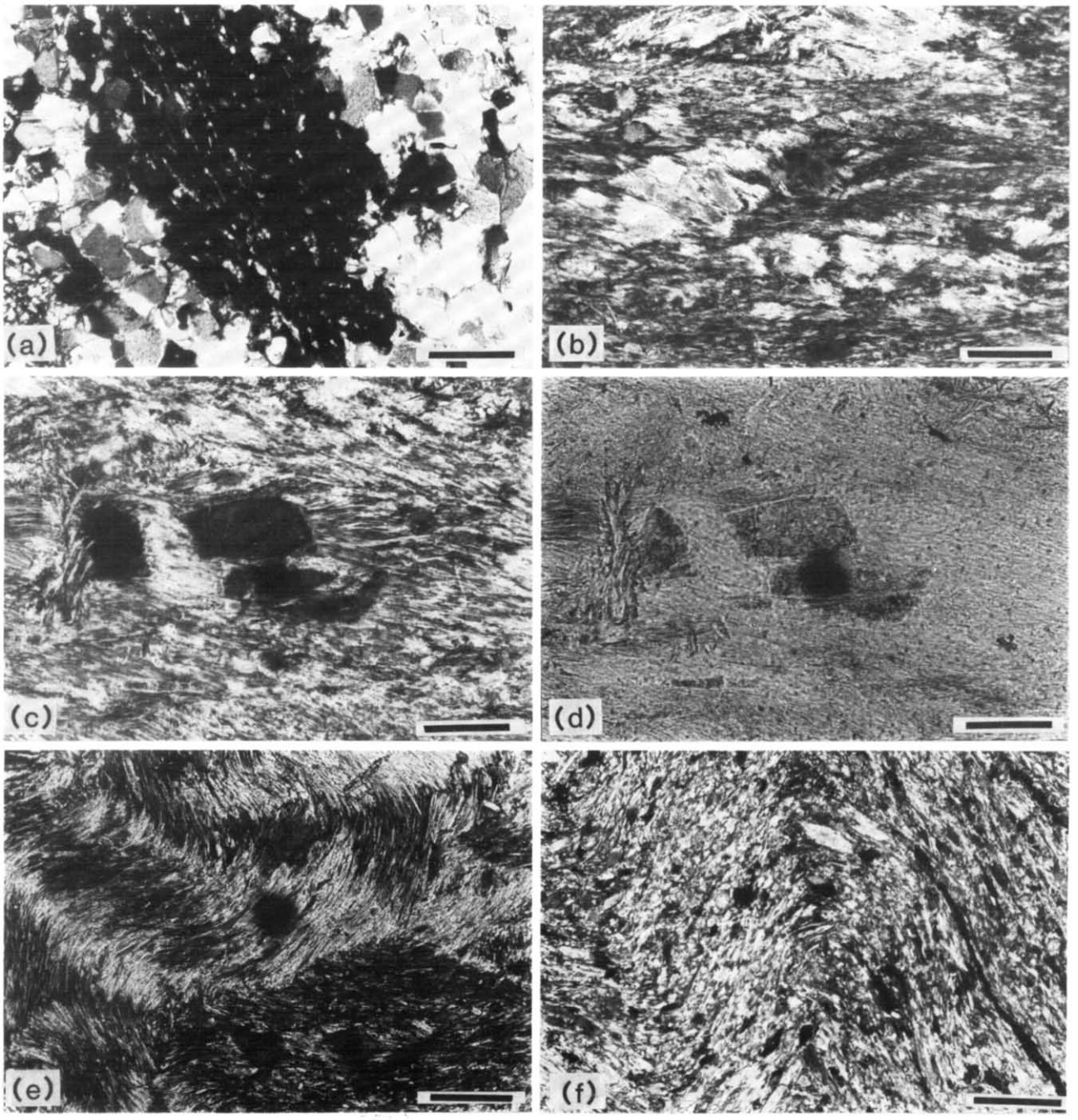

Fig. 5. (a) Olivine poikiloblast (at extinction) containing inclusions of tremolite needles which define a straight S_i in a type 2 ultramafite. S_i is parallel to the external foliation (S_m) which is defined by elongate poikiloblasts and by banding of tremolite and chlorite (not visible in figure). The olivine poikiloblast is surrounded by a mosaic of tremolite which contrasts markedly with the inclusions. Scale bar is 0.2 mm. (b) Fractured tremolite porphyroclasts in a matrix of acicular tremolite. Note the weakly asymmetric pattern defined by the prominent porphyroclast and overgrowths in the left portion of the figure. Overgrowths on porphyroclasts are parallel to S_m. Scale bar is 0.2 mm. (c) Separated tremolite porphyroclast connected by curved tremolite fibers in a type 3 ultramafite. The fibers may have grown in pressure shadows with concomitant rotation of the fragmented porphyroclast. Minor chlorite has grown transverse to S_m. Scale bar is 0.1 mm. (d) Same as (c), but in plane light. Note the turbid porphyroclasts, their clear rims, and the fibrous overgrowths. Scale bar is 0.1 mm. (e) Post-crystalline microfolds in a mylonitic, tremolite-rich type 3 ultramafite. Note that overgrowths on the porphyroclast in the center of the figure (at extinction) are folded. Note also the porphyroclast in the lower portion of the figure which has been separated into two fragments connected by fibrous tremolite. Scale bar is 0.1 mm. (f) Polygonal arc in a tremolite-rich type 3 ultramafite indicating syn- to post-tectonic recrystallization of tremolite. Scale bar is 0.2 mm.

exposed thickness of the ophiolite a few km to the south of the roof pendant in the main outcrop area of the Ingalls Complex (Miller 1985). A maximum of about 500 MPa is probable if the upper plate consists mostly of oceanic crust of normal thickness, but thickened somewhat by imbrication, and of several km of the uppermost mantle.

Assemblages in metabasites and metasedimentary rocks are also consistent with temperatures of mid-amphibolite facies or higher. Epidote is absent in the amphibolites, which consist of hornblende–plagioclase (andesine to labradorite) ± diopside ± cummingtonite ± biotite ± quartz ± sphene. Metasedimentary rocks generally contain quartz-biotite ± cummingtonite ± hornblende ± garnet ± plagioclase.

MICROSTRUCTURES

Complex microstructures were produced in the ultramafic rocks as a result of at least two major metamorphic events—pre-emplacement, 'mantle event(s)' (Miller 1985) and the later, syn-thrusting, amphibolite-facies event. Microstructures which probably formed during the 'mantle event(s)' are preserved in the interiors of the thickest slices. These peridotites are invariably type 1 in composition, whereas all three types record the amphibolite-facies event.

The 'mantle rocks' are generally coarser-grained and display a weaker foliation than the other ultramafites. Textures in the 'mantle rocks' range from sub-equigranular to porphyroclastic (Fig. 4c). Olivine porphyroclasts (2–3 mm long) display well-developed deformation bands and subgrains. Neoblasts are commonly 0.2–0.4 mm in length. Foliation (S_1; Table 1) is defined by weakly elongate porphyroclasts and spinel aggregates. Enstatite is subhedral to euhedral and ranges from medium- to coarse-grained. Some orthopyroxene is unstrained, but subgrains, deformation bands, kink bands and bent grains also are present. Neoblasts locally help define a 'core and mantle' structure. In some of the 'mantle rocks', fibrous talc, chlorite and tremolite form pseudomorphs after pyroxenes. These replacement products contrast with the well-recrystallized tremolite and talc which are part of the equilibrium assemblage in the mylonitic type 1 ultramafites described below.

Microstructures related to the syn-thrusting amphibolite-facies event are unevenly developed in type 1 ultramafites, and in many samples it is difficult to distinguish textures of this event from those formed by the 'mantle' event. Samples collected from foliated (S_m, S_2) zones which clearly cut the 'mantle' fabric are characterized by a polygonal mosaic. Olivine (0.1–0.2 mm) and relict chromite are much finer-grained than in adjacent 'mantle' rocks. Bands of olivine mosaic commonly alternate with layers of aligned tremolite and/or fine-grained (0.15 mm), equigranular talc in strongly foliated (S_2, S_m) samples. Olivine porphyroclasts, displaying prominent subgrains, also occur in some mylonitic type ultramafites.

Orthopyroxene locally occurs in mylonitic type 1 ultramafites where within an individual sample it shows two types of textures. Some enstatite forms a fine-grained equigranular mosaic with olivine, but other enstatite occurs as coarser-grained poikiloblasts with inclusions of olivine. These textures are in marked contrast to those of the orthopyroxenes in the 'mantle-type' rocks.

Olivine textures are considerably more variable in the type 2 ultramafites than in the type 1 rocks. Olivine is darkened by magnetite granules in numerous samples, in contrast with the local occurrence of such olivines in the type 1 rocks. Porphyroclastic textures dominate a few of the type 2 ultramafites. Olivine porphyroclasts display subgrains, and neoblasts average about 0.1 mm in length. Elongate tremolite, which defines S_m, wraps around lenses of olivine and is recrystallized.

Some nearly equigranular type 2 ultramafites are characterized by banding (1–2 mm) of olivine and tremolite (Fig. 4d). Most olivine forms a fine-grained (0.1–0.3 mm) polygonal mosaic, but local porphyroclasts display subgrains. Tremolite is also well-recrystallized and elongate grains wrap around local lenses of olivine. Green spinel occurs in a few samples as granules within olivine and as larger, weakly elongate grains which help define S_m.

Distinctive markedly elongate olivine characterizes other type 2 ultramafites. These olivines attain 8.0 mm in length and grains with aspect ratios of about 6 : 1 to 7.5 : 1 occur in several samples. In some rocks, olivine occurs almost exclusively as elongate grains, whereas in others it also forms a fine-grained mosaic. The elongate grains are generally unstrained, and many are extremely poikiloblastic. Inclusions of tremolite and chlorite needles, and rarely of spinel granules, commonly define a straight internal fabric (S_i) (Fig. 5a) which is parallel to the external foliation (S_m). Inclusions also define rare microfolds within the olivines, and a chlorite-defined microfold was seen within a large, post-kinematic tremolite.

Tremolite defines S_m and is generally well-recrystallized in the samples containing elongate olivine. The tremolite fabric is not deflected by the elongate olivine, and, in a few places, elongate grains appear to cut S_m. Acicular grains of amphibole are common in some samples, where they locally define microfolds. In other samples, however, they occur only as inclusions in olivine, where they presumably were spared from the extensive recrystallization and grain growth that affected the other tremolite. The textural relationships between olivine and tremolite in the type 2 ultramafites are compatible with two stages of growth of both phases. In the porphyroclastic samples olivine apparently was extensively recrystallized during mylonitization. Tremolite was deformed around the olivine porphyroclasts, but also recrystallized. Elongate forsterite provides evidence for a second stage of olivine growth. The lack of deflection of the mylonitic fabric by these olivines, the parallelism of the internal fabric and S_m, and the absence of strain in markedly elongate grains all indicate that

these olivines are late- to post-kinematic. Elongate olivines in general are apparently best developed during static amphibolite-facies metamorphism (cf. Evans & Trommsdorff 1974, Snoke & Calk 1978). The contrast between the acicular tremolite preserved in olivine poikiloblasts and the generally coarser, less elongate tremolite that dominates these rocks also indicates two stages of tremolite growth. The variable ratio and gradation of acicular to coarser grains in some poikiloblastic samples suggest that these stages represent the extremes of a continuum, rather than two distinct events.

The amphibole-rich mylonitic type 3 ultramafites (tremolitites) share some microstructures with the type 2 rocks. Foliation (S_m) in both types is defined by orientated tremolite, grain-size layering, layering marked by variations in preferred orientation of tremolite and spinel aggregates.

Several stages of tremolite growth have also been recognized in the type 3 ultramafic rocks. The earliest stage is only locally preserved (<25% of the tremolites) by fine- to medium-grained (0.3–1.8 mm) porphyroclasts which occur in a fine-grained matrix of acicular tremolite. Some of these porphyroclasts conceivably were originally pseudomorphs after pyroxene. Porphyroclasts range from blocky to strongly elongate, with aspect ratios reaching 4.5:1, and most are aligned in S_m. The larger porphyroclasts are commonly bent and broken (Fig. 5b–d); some have been separated into numerous fragments. Shear microfractures oriented parallel to cleavage planes and extensional microfractures subnormal to S_m occur in about equal numbers. The porphyroclasts generally display patchy undulose extinction. Opaque granules impart a turbid appearance to many of the larger porphyroclasts and a few of the smaller grains (Fig. 5d).

The second stage of tremolite growth is recorded by strongly aligned acicular crystals which are the most abundant grains in the mylonitic type 3 ultramafites. Some samples consist almost entirely of acicular tremolite. In porphyroclastic tremolites, acicular (fibrous) grains occur as overgrowths on tremolite porphyroclasts and connect fragments of broken porphyroclasts (Fig. 5b–e).

There are no consistent crystallographic relationships between porphyroclasts, their rims, and fibrous overgrowths. In some, generally larger, porphyroclasts, turbid cores are surrounded by thin clear rims which typically have an obviously different optic orientation (Fig. 5c, d). Narrow clear patches locally penetrate from rims into turbid cores along fractures. Some rims are in optical continuity with overgrowths, but only rarely are cores, rims and overgrowths all optically continuous. In turbid porphyroclasts lacking rims, optical continuity of overgrowths is also rare. Continuity of overgrowths on small, non-turbid porphyroclasts is more common, but still subordinate. Local turbid microboudinaged porphyroclasts have been separated into fragments which are connected and enclosed by non-fibrous tremolite that forms an optically continuous rim.

Both acicular grains connecting porphyroclast fragments and fibrous crystals in overgrowths lie parallel to S_m. Thus, these syntectonic fibrous amphiboles probably record the direction of maximum extension. Fibers in overgrowths also commonly are strongly curved and/or folded (Fig. 5e). The sweeping extinction of the fibers indicates that the curvature resulted from later deformation, rather than being solely an artefact of growth during non-coaxial extension. Locally, overgrowths and fibers connecting fragments of separated porphyroclasts define an asymmetric augen-like microstructure. Post-crystalline crenulations marked by bent acicular grains are common in the type 3 tremolitites (Fig. 5e), and to a lesser extent in the type 2 ultramafites, as are fine- to locally medium-grained polygonal arcs (Fig. 5f). These microfolds are asymmetric, open to tight, disharmonic and commonly chaotic. An approximately axial-planar, anastomosing spaced foliation (S_3) is defined by fold limbs and/or discrete zones of orientated tremolite; it is rarely the dominant foliation. Other acicular tremolites are parallel to fold axes.

In some of the type 3 ultramafites, elongate tremolite porphyroclasts and their overgrowths are bent into microfolds (Fig. 5e). By contrast, other, generally small porphyroclasts apparently acted as rigid inclusions during folding and somewhat disrupted the forms of nearby microfolds.

There is local gradation within individual samples of type 2 and type 3 ultramafites from the acicular grains into medium-grained, weakly to moderately elongate tremolite. These latter tremolites generally are moderately strongly aligned, possibly as a result of mimetic growth, and locally form polygonal arcs. The latest stage of tremolite growth is recorded sporadically by post-kinematic, fine- to medium-grained crystals which have grown across S_m.

A few of the tremolitites do not readily fit into this textural sequence. They consist mainly of a fine- to medium-grained, equigranular mosaic of equant or weakly elongate crystals.

Granules of chromite typically form discontinuous trains and layers parallel to S_m in the type 2 and type 3 rocks. Medium-grained, euhedral, elongate chromite persists in some mylonites.

DEFORMATION MECHANISMS

Mylonitization was accomplished on the microscale mainly by deformation of olivine and tremolite. In mylonitic type 1 ultramafites the combination of widespread subgrains and recrystallized grains of olivine indicates that dislocation creep was the dominant deformation mechanism. The fine grain size of olivine suggests that this episode of dislocation creep occurred at considerably higher stresses than the earlier 'mantle-type' deformation.

Deformation of the type 2 ultramafites was more complex, as both olivine and tremolite are common in these rocks. Olivine microstructures in some of these ultramafites are similar to those in the mylonitic type 1

rocks and indicate dislocation creep. The mechanism operative during tremolite deformation is less clear. The abundance of strongly aligned acicular tremolite in both the type 2 and type 3 rocks suggests a common deformation mechanism.

Porphyroclasts of tremolite in the mylonitic type 3 ultramafites preserve a record of early amphibole deformation which is absent in the type 2 ultramafites. Porphyroclasts apparently deformed mainly by microfracturing, as indicated by the abundance of broken grains combined with the scarcity of subgrains and related recrystallized grains. Microfracturing led to considerable grain size reduction. The larger porphyroclasts commonly have been separated into several fragments by extension and shear microfractures, whereas many of the smaller porphyroclasts are not fractured. Undulose extinction and less common deformation bands in porphyroclasts may record minor intracrystalline deformation prior to microfracturing.

Formation of fibrous tremolite overgrowths on porphyroclasts probably accompanied cataclasis. Interpretation of overgrowth microstructures in mafic and ultramafic rocks is generally complicated, as it is commonly difficult to establish whether overgrowths are syntectonic or post-tectonic (Brodie & Rutter 1985). Recrystallization and grain growth have obscured overgrowth–porphyroclast relationships in many of the tremolitites. Nevertheless, syntectonic growth is implied by the strong alignment parallel to S_m of fibrous tremolite in overgrowths. Fibers clearly did not simply grow randomly into fluid-filled voids. Rare examples of paracrystalline microboudinage also demonstrate syntectonic growth (cf. Misch 1969).

The general lack of optical continuity of clear rims and fibrous overgrowths with turbid cores suggests a changing composition of clinoamphibole during deformation and may reflect a type of incongruent pressure solution (cf. Beach 1982) or precipitation from an evolved fluid. LaTour & Kerrich (1982) similarly have drawn an analogy between amphibole overgrowths on amphibole porphyroclasts with mica and chlorite beards formed during pressure solution.

Thus overgrowths probably record syntectonic growth of fibrous tremolite into dilatant microfractures during diffusive mass transfer which accompanied cataclasis (cf. Brodie & Rutter 1985, Rutter *et al.* 1985). Growth presumably occurred on surfaces of low normal stress. The dominance of acicular tremolite in type 3 ultramafites may reflect the pervasiveness of diffusive mass transfer. The abundance of acicular grains in some type 2 ultramafites suggests that tremolite deformed by similar mechanisms in these rocks.

Other mechanisms possibly played lesser roles in the deformation of the tremolitic rocks. Grain boundary sliding commonly accommodates cataclasis and diffusive mass transfer (e.g. Rutter *et al.* 1985), but the importance of this mechanism in the tremolitic rocks is difficult to assess. Evidence for dislocation creep in tremolite is weak. A few samples consisting entirely of a fine- to medium-grained mosaic of equant to weakly elongate tremolite conceivably experienced pervasive dynamic recrystallization. Alternatively, this mosaic may simply have resulted from annealing of cataclastic tremolite. Coarsening of amphibole by secondary grain growth occurred in some tremolitic rocks and obscured the earlier microstructural history.

Experimental and microscopic studies of amphibole deformation are incomplete in comparison to other important minerals. Nevertheless, the observations of the tremolitic rocks are in general agreement with previous studies that have stressed the importance of cataclastic deformation of amphibole (e.g. Allison & LaTour 1977, Brodie & Rutter 1985) and have shown that fibrous amphibole overgrowths commonly accompany microfracturing (e.g. LaTour & Kerrich 1982, Rutter *et al.* 1985).

Overgrowth relationships in the tremolitites may have implications for amphibole deformation in general. Brodie & Rutter (1985) in their summary of deformation in basic rocks emphasize that in prograde rocks reactions typically go to completion and destroy overgrowth textures; thus, preserved overgrowths generally occur in retrograde shear zones. Overgrowths in the type 3 ultramafites, however, may not be simply late retrograde features. Many of the fibrous tremolites in overgrowths in these ultramafites are strongly deformed. Some bent grains define microfolds, and others have recrystallized at the same time as, or subsequent to, folding, and form polygonal arcs. The occurrence of acicular tremolite grains within olivine, including those which define a helicitic texture (see above), suggests continuation of amphibolite-facies conditions after formation of the overgrowths. Furthermore, although tremolite can form under greenschist-facies conditions, it is not clear whether the overgrowths formed at lower temperatures than the porphyroclasts. The overgrowths may have slightly different compositions than the porphyroclasts, but they are both identified optically as tremolite. Perhaps the overgrowths may be explained by deformation under relatively constant temperatures, but with diffusive mass transfer occurring as a result of reduced stress and strain rate, and/or as a result of reduced grain size by microfracturing.

A problem may exist in reconciling the deformation mechanisms interpreted for tremolite with the dislocation creep apparently recorded by olivine. At low strain rates, olivine deforms by dislocation creep at a temperature of >700°C (e.g. Kirby 1983, 1985, Chopra & Paterson 1984) which is near the upper limit permitted by metamorphic assemblages in the imbricate zone. In contrast, flow dominated by diffusive transfer plus grain boundary sliding and microfracturing is important in amphiboles at least to lower amphibolite-facies conditions (LaTour & Kerrich 1982). Dislocation creep apparently becomes significant in amphibole deformation at temperatures of >600°C in mafic rocks (Dollinger & Blacic 1975, Nielsen 1978, LaTour & Kerrich, 1982).

The discrepancy in estimated temperatures for the inferred deformation mechanisms of olivine and tremolite may be interpreted in several ways. One explanation

is that tremolite experienced later deformation than olivine and at lower temperatures. This interpretation is permissible for the type 3 ultramafites and is compatible with the range of temperatures apparently recorded by the type 1 and type 2 ultramafites. However, the occurrence of acicular tremolite inclusions within olivine indicates that amphibolite-facies conditions continued after formation of the amphiboles in the type 2 rocks (see above), and the equilibrium textures of olivine and tremolite also argue against this interpretation (Figs. 4d and 5a).

A second explanation is that tremolite deformed by microfracturing and diffusive mass transfer at higher than expected temperatures (>600°C). The combination of several factors may have favored microfracturing and diffusive creep at the expense of dislocation creep. Diffusive mass transfer can operate at relatively high temperatures under low stresses and strain rates. High fluid pressures, which probably occurred during deformation (see below), favor cataclasis and diffusive transfer. Microfracturing led to marked refinement of porphyroclasts, and the very fine grain sizes of tremolite also presumably enhanced diffusive mass transfer.

A third possibility is that olivine deformed by dislocation creep at temperatures of <700°C. Temperatures for dislocation creep are lower for wet olivine than for dry olivine (Kirby 1985). The abundant hydrous phases in the type 2 ultramafites suggest that the lower T experimental curves for wet olivine (e.g. Chopra & Paterson 1984) may be applicable for these rocks. High deviatoric stresses might also have sufficiently lowered the temperatures needed for dislocation creep in olivine. The fine grain size of olivine in some type 1 and type 2 ultramafites is compatible with such stresses.

In summary, although there is no unequivocal explanation of the apparent problem posed by the deformation mechanisms in olivine and tremolite, I tentatively suggest that high fluid pressures, of which there is considerable evidence, were partly responsible for microfracturing of amphibole and diffusive transfer at relatively high temperatures (>600°C). Furthermore, dislocation creep in olivine and diffusive mass transfer in amphibole may have alternated in a cyclic fashion with the latter occurring during periods of reduced stress.

FORMATION OF THE METASOMATIC ROCKS

Tremolitic and chloritic rocks are common in metasomatized ultramafic bodies. The nature of the ultramafic protolith(s) is important for the interpretation of the evolution of the mylonites. It is particularly important whether the protolith was anhydrous peridotite or serpentinite.

Indirect evidence of a mixed peridotite and serpentinite protolith is provided from a large, structurally higher outcrop area of the Ingalls Complex south of the imbricate zone which escaped the amphibolite-facies metamorphism (Fig. 1) (Miller 1985) and lacks obvious thrust-related structures. In this area, cm^2- to km^2-sized blocks of harzburgite and lherzolite, and sedimentary and mafic ophiolitic rocks, are enclosed in a sheared serpentinite matrix. Zones of serpentinite matrix range from <1 m to >1 km in width. Tectonic mixing probably occurred in an oceanic fracture zone prior to imbrication and the amphibolite-facies event (Miller 1985).

There also is evidence in the imbricate zone for both a peridotite and serpentinite protolith. Evidence of a peridotite parent includes preservation of the premylonitic, 'mantle-type' assemblage forsterite–enstatite–spinel and medium- to coarse-grained porphyroclastic olivine textures in weakly deformed portions of ultramafic slices. Podiform chromite bodies also occur locally. In contrast, abundant magnetite granules included in forsterite grains in some type 2 and a few type 1 ultramafites suggest that these olivines were regenerated from serpentine (Vance & Dungan 1977). Stringers of magnetite which help define S_m in some mylonites may be relics from sheared serpentinite. Furthermore, some type 3 rocks consist solely of acicular tremolite which defines an anastomosing fabric reminiscent of foliated serpentinite and possibly formed by replacement of fibrous serpentine. The presence of metarodingite containing the assemblage zoisite–clinozoisite–diopside–grossularite also indicates serpentinization prior to amphibolite-facies metamorphism. In summary, both serpentinite and peridotite were present prior to metamorphism, but their relative proportions as protoliths for the metasomatic rocks, as well as for type 1 ultramafites, are poorly known.

A comparison of the mineralogy of the metasomatic rocks and their protoliths allows a simple qualitative determination of ionic transfer during metasomatism. Hydration of peridotite to produce a tremolitic rock requires addition of Ca^{2+} and Si^{4+} and the release of Mg^{2+} into the fluid phase. The amount of Ca^{2+} is clearly dependent partly on whether the peridotite was harzburgite or lherzolite. Conversion of serpentinite to tremolitite involves addition and removal of the same ions, but also releases relatively large quantities of water.

Similar considerations show that the formation of chloritic rock by hydration of peridotite requires addition of Al^{3+} and removal of Mg^{2+}. Conversion of serpentine to chlorite also clearly involves introduction of Al^{3+} and release of Mg^{2+} and Si^{4+}.

The scarcity of carbonate-bearing assemblages in the ultramafites suggests that the fluid phase was almost entirely water. Some internal metasomatic zones are greater than 25 m from the nearest non-ultramafic rocks, the presumed source of the introduced ions. This scale of metasomatism indicates that infiltration (advection) of an ionic metasomatic fluid was much more important than diffusion through a stationary fluid under a chemical-potential gradient. Infiltration can occur on a large scale (cf. Etheridge *et al.* 1984), whereas diffusion generally operates over only short distances (<1 m) (Fletcher & Hoffman 1974, Rohr 1985). Extensive dilation, attested to by widespread veining, was ideal for infiltration. Diffusion may have played a minor role by modify-

ing the initial boundaries of the infiltration-induced internal metasomatic zones (cf. Fletcher & Hoffman 1974, Rohr 1985), and may also have had a small role in the formation of marginal mylonite zones.

FLUID FLOW IN THE IMBRICATE ZONE

Large volumes of fluid probably infiltrated the ultramafic rocks with flow mainly focused along structural channelways. Ubiquitous tremolite veins provide evidence of narrowly channelized fluid flow, whereas mylonitic type 2 and type 3 metasomatic ultramafites record more pervasive flow.

Subnormal extensional tremolite veins in the imbricate zone may have formed by hydraulic fracturing and suggest that fluid pressures at least periodically exceeded the sum of the least compressive stress and the tensile strength of the rock (e.g. Secor 1965). High fluid pressures are probably particularly necessary to develop pervasive veining in the medium-grade rocks of the imbricate zone. The postulated hydraulic fracturing may have been facilitated by the inability of fluid loss through pores to keep up with fluid production by devolatization reactions (e.g. Yardley 1983, 1986, Murrell 1985). Hydraulic fracturing, in turn, would have significantly increased permeability, thereby reducing fluid pressures. The numerous generations of tremolite veins, showing variable degrees of deformation and recrystallization, are compatible with fluctuating fluid pressures during deformation, possibly related to varying permeability and/or a cyclic build-up and release of pore fluids (cf. Murrell 1985, Yardley 1986).

The high fluid pressure and fluid flux postulated for the imbricate zone presumably resulted from devolatization reactions. If some of the type 1 ultramafites were serpentinites prior to amphibolite-facies metamorphism, then considerable water may have been released by the breakdown of serpentine to forsterite plus talc. In experiments, this dehydration reaction raises fluid pressures and lowers effective stresses, leading to weakening and embrittlement (Raleigh & Paterson 1965). Prior to imbrication and metamorphism the ultramafites probably consisted of a mixture of serpentinite and anhydrous 'mantle-type' peridotite; thus, there existed both a source and a sink for fluids. In a sense, prograde dehydration of serpentinite may have resulted in retrogressive hydration of the 'mantle-type' peridotites.

Although dehydration of serpentinite may have provided much fluid, it could not be totally responsible for fluid flow in the ultramafites. The preponderance of tremolite in veins and mylonite zones indicates the importance of the activities of calcium and silicon ions in the infiltrating fluid. The breakdown of serpentine could not yield the Ca^{2+} and Si^{4+} necessary to produce tremolite from peridotite. Moreover, some tremolitites may be transformed serpentinites and an external source of Ca^{2+} and Si^{4+} is clearly required.

Amphibolite, orthogneiss and metasedimentary slices in the imbricate zone are other possible sources for the fluids that flowed through the ultramafites. Prograde metamorphism of amphibolites and metasedimentary rocks characteristically results in devolatization; as the amphibolites are more abundant, I will base the following interpretative discussion on them. The protoliths of at least many of the amphibolites were ophiolitic gabbros, diabases and basalts that experienced ocean-floor-type metamorphism; thus they consisted mostly of greenschist-facies assemblages prior to the amphibolite-facies event (Miller 1985). During the latter metamorphism, the formation of hornblende, presumably at the expense of chlorite, together with the breakdown of epidote, resulted in significant devolatization of the mafic rocks. These devolatization reactions should have raised fluid pressures, thus greatly increasing permeability (e.g. Brace 1972, Rumble *et al.* 1982, Ferry 1983) and enabling fluids to migrate through and out of the amphibolites. Some of the fluids generated by these reactions presumably flowed into nearby ultramafic slices, and probably provided Ca^{2+} and Si^{4+} necessary for the metasomatic tremolite. Ca^{2+} may also have been supplied by mafic rocks rodingitized during early serpentinization.

The relative distribution of type 2 and type 3 ultramafites may be relevant to these interpretations. The coexistence of forsterite and tremolite in type 2 ultramafites, the dominant constituents of internal zones, suggests that Ca^{2+} ions were not present in excess and that the activity of Ca^{2+} played a role in reactions in these zones. Conversely, abundant tremolitites indicate that excess Ca^{2+} was generally present in the marginal zones. These relationships possibly reflect the greater distances (reduced Ca^{2+} concentrations?) for mass transport from amphibolite slices to internal metasomatic zones.

Fluids generated in amphibolites and metasedimentary rocks evidently infiltrated ultramafites for distances of at least tens of meters in order to metasomatize some of the internal mylonite zones. However, fluid transport did not necessarily exceed 100 m owing to the thinness of most imbricate slices.

The rate of fluid production in the metabasites may have been fairly constant, but perhaps punctuated periodically by 'dehydration bursts' (Fyfe 1976), as both continuous and discontinuous reactions characterize prograde metamorphism (e.g. Carmichael 1969, Etheridge *et al.* 1983). The presence of numerous generations of tremolite veins, showing varying degrees of deformation and recrystallization (see above), may result from fluctuating, but overall relatively persistent fluid production. By contrast, in the ultramafites with a postulated serpentinite protolith the breakdown of serpentine was probably a discontinuous reaction that may have resulted locally in unusually elevated fluid pressures for a short period of time.

SUMMARY OF RELATIONSHIPS AMONG METAMORPHISM, FLUID FLOW AND DEFORMATION

The concentration of mylonitization in tremolitic rocks suggests a genetic relationship between meta-

morphism and deformation in the imbricate zone. A key problem is determining when metasomatism occurred during the deformational history of the ultramafic rocks. This is a common problem in shear zones as it is often difficult to establish whether hydration and metasomatism accompanied mylonitization, or occurred after deformation and simply utilized pre-existing mylonite zones (*cf.* Brodie & Rutter 1985). It is clear, however, that in the Ingalls Complex there was significant deformation at the same time as or subsequent to metamorphism. This problem is addressed in the following attempt to integrate the larger-scale structural evolution of the Ingalls Complex with the smaller-scale structural and metamorphic history.

Initial deformation of the Ingalls Complex probably occurred in an oceanic fracture zone (Miller 1985, Miller & Mogk 1987). Movements in this zone led to mixing of hydrothermally metamorphosed mafic igneous rocks and sedimentary rocks with variably serpentinized ultramafic rocks. The resultant rock assemblage contained large zones of serpentinite mélange.

Thrust emplacement of these ophiolitic rocks at a continental margin apparently resulted in further mixing along imbricate faults and the ophiolite was also imbricated with the Heterogeneous Metamorphic Suite (see above). It is not clear whether initial imbrication occurred under amphibolite-facies conditions or at lower temperatures where new zones of sheared serpentinite may have formed. In either case, the imbrication and earlier tectonic mixing in the fracture zone probably had a major influence on metasomatic fluid flow. Faulting juxtaposed contrasting rock types that were potential sources and sinks for metasomatic fluids. The spacing of faults influenced the abundance of metasomatic rocks within a given rock volume; metasomatic mylonites are scarce within the thickest metaperidotite slices.

The mechanism by which the shear zones associated with the imbricate thrusts were initiated and developed is unknown as the mylonites were metasomatically hydrated prior to, or at the same time as, the microstructures now observed. Microfracturing is the earliest mechanism recognized in the tremolitites, and even earlier cataclasis would have led to dilatancy and allowed fluids access to the ultramafic protolith as the shear zone developed (e.g. Beach 1973).

The infiltration of fluids to form the abundant tremolite veins and metasomatic zones may have either accompanied initial imbrication or occurred after a time interval of unknown length. By the time infiltration occurred, temperatures apparently were in the amphibolite facies. Infiltration was probably enhanced by the relatively fine grain size and strong anisotropy produced by deformation in the mylonite zones. The importance of these structural channelways is clear, regardless of whether they were initially zones of sheared serpentinite or formed at higher temperatures. The former zones would have been particularly favorable pathways for fluid transport.

Deformation at the same time as(?) and subsequent to formation of the type 2 and type 3 ultramafites was localized predominantly in these metasomatic zones. The variable deformation of tremolite veins, from incipient to mylonitic, suggests that mylonitization occurred while fluid fluxes were still high. This interpretation seems particularly plausible if some of the monomineralic layers and gneissic bands of tremolite alternating with olivine-rich bands are strongly deformed veins (see above).

The softening indicated by localization of the latest strains in tremolitic mylonites may have resulted from several factors. Deformation by microfracturing and diffusive mass transfer of tremolite was apparently easier generally than deformation by dislocation creep or other mechanisms in olivine-rich rocks. The concentration of deformation in metasomatic zones may have been controlled by localized zones of high pore pressure. High fluid pressures may have promoted microfracturing, and a high fluid flux would also have favored diffusive transfer. Microfracturing reduced grain size, thus further favoring diffusive mass transfer, and a decrease in stress and strain rate would also have had the same effect. The change to diffusive mass transfer as the deformation mechanism is capable of producing significant softening (Rutter 1976, White *et al.* 1980). If dislocation creep had dominated, then it seems unlikely that strain would have been concentrated in amphibole-rich rocks, which tend to be strong under conditions of the middle amphibolite facies and lower temperatures.

GENERAL IMPLICATIONS OF THE METASOMATIC MYLONITES

Infiltrating metasomatic fluids probably play an important role in the evolution of shear zones in many ultramafic bodies during medium-grade metamorphism. Focused fluid flow along structural and lithologic channels should be common in ultramafites. Many alpine peridotites are variably serpentinized and cut by shear zones prior to or at the same time as their emplacement into orogenic belts; the result is a structurally anisotropic mixture of rocks showing varying degrees of hydration. Therefore, fluid production during any subsequent medium- to high-grade metamorphism will be markedly heterogeneous. Large gradients in fluid pressure and permeability may result, and they in turn may lead to focused fluid flow.

The infiltrating fluids may include components derived by devolatization of adjacent non-ultramafic rocks; metasomatism of ultramafites typically results. This process is presumably widespread in medium- to high-grade metamorphic belts, as metaperidotites commonly occur as pods and slices intimately interleaved with metabasites and metasedimentary rocks. Evidence for metasomatism does indeed occur in numerous orogens; monomineralic zones commonly form at contacts of greenschist- and amphibolite-facies metaperidotites (e.g. Chidester 1962, Jahns 1967) and internal metasomatic zones have also been reported (e.g. Jahns 1967, Misch 1977, Brodie 1980). However, other examples of

interrelated metasomatism and mylonitization in medium- to high-grade ultramafic rocks have rarely been reported. It may be that the significance of infiltrating metasomatic fluids during deformation of ultramafic rocks in some other terrains has not been recognized, perhaps because of the obscuring effect of later serpentinization.

Acknowledgements—I thank D. Borns, R. Frost, D. Mogk, K. Nielsen and S. Paterson for their comments on early versions of this manuscript, and P. Hudleston and the anonymous reviewers of the Journal for their constructive criticisms. Initial field work was supported by Geological Society of America Penrose Grants, Sigma Xi, and a University of Kansas Faculty Research Grant.

REFERENCES

Allison, I. S. & LaTour, T. E. 1977. Brittle deformation of hornblende in a mylonite: A direct geometrical analogue of ductile deformation by translation gliding. *Can. J. Earth Sci.* **14**, 1953–1959.

Beach, A. 1973. The mineralogy of high temperature shear zones at Scourie, N.W. Scotland. *J. Petrology* **14**, 231–248.

Beach, A. 1976. The interrelations of fluid transport, deformation, geochemistry and heat flow in early Proterozoic shear zones in the Lewisian complex. *Phil. Trans. R. Soc. Lond.* **A280**, 590–604.

Beach, A. 1980. Retrogressive metamorphic processes in shear zones with special reference to the Lewisian complex. *J. Struct. Geol.* **2**, 257–263.

Beach, A. 1982. Deformation mechanisms in some cover thrust sheets from the external French Alps. *J. Struct. Geol.* **4**, 137–149.

Borges, F. S. & White, S. H. 1980. Microstructural and chemical studies of sheared anorthosites, Roneval, South Harris. *J. Struct. Geol.* **2**, 273–280.

Brace, W. F. 1972. Pore pressure in geophysics. In: *Flow and Fracture of Rocks* (edited by Heard, H. C., Borg, I. Y., Carter, N. L. & Raleigh, C. B.). *Am. Geophys. Union Geophys. Monogr.* **16**, 265–273.

Brodie, K. H. 1980. Variations in mineral chemistry across a shear zone in phlogopite peridotite. *J. Struct. Geol.* **2**, 265–272.

Brodie, K. H. & Rutter, E. H. 1985. On the relationship between deformation and metamorphism with special reference to behavior of basic rocks. In: *Advances in Physical Geochemistry, Vol. 4. Metamorphic Reactions: Kinetics, Textures and Deformation* (edited by Thompson, A. B. & Rubie, D. C.). Springer, Berlin, 138–179.

Carmichael, D. M. 1969. On the mechanism of prograde metamorphic reactions in quartz-bearing pelites. *Contr. Miner. Petrol.* **20**, 244–267.

Chernosky, J. V. 1976. The stability of anthophyllite—a re-evaluation based on new experimental data. *Am. Miner.* **61**, 1145–1155.

Chidester, A. H. 1962. Petrology and geochemistry of selected talc bearing ultramafic rocks and adjacent country rocks in north-central Vermont. *Prof. Pap. U.S. geol. Surv.* **345**, 207.

Chopra, P. N. & Paterson, M. S. 1984. The role of water in the deformation of dunite. *J. geophys. Res.* **89**, 7861–7876.

Dollinger, G. & Blacic, J. D. 1975. Deformation mechanisms in experimentally and naturally deformed amphiboles. *Earth Planet. Sci. Lett.* **26**, 409–416.

Engels, J. C. & Crowder, D. F. 1971. Late Cretaceous fission-track and potassium–argon ages of the Mount Stuart granodiorite and Beckler Peak stock, North Cascades, Washington. *Prof. Pap. U.S. geol. Surv.* **750**, D39–D43.

Etheridge, M. A., Wall, V. J. & Vernon, R. H. 1983. The role of the fluid phase during regional metamorphism and deformation. *J. Metamorphic Geol.* **1**, 205–236.

Etheridge, M. A., Wall, V. J. & Cox, S. F. 1984. High fluid pressures during regional metamorphism and deformation: Implications for mass transport and deformation mechanisms. *J. geophys. Res.* **89**, 4344–4358.

Evans, B. W. 1982. Amphiboles in metamorphosed ultramafic rocks. In: *Reviews in Mineralogy, 9A, Amphiboles and Other Hydrous Pyriboles-Mineralogy* (edited by Veblen, D. R. & Ribbe, P. H.), 98–112.

Evans, B. W. & Trommsdorff, V. 1974. On elongate olivine of metamorphic origin. *Geology* **2**, 131–132.

Evans, B. W., Johannes, J., Oterdoom, H. & Trommsdorff, V. 1976. Stability of chrysotile and antigorite in the serpentinite multisystem. *Schweiz. miner. petrogr. Mitt.* **50**, 481–492.

Ferry, J. M. 1983. Regional metamorphism of the Vassalboro Formation, south-central Maine, U.S.A.: a case study of the role of fluid in metamorphic petrogenesis. *J. geol. Soc. Lond.* **140**, 551–576.

Fletcher, R. C. & Hoffman, A. W. 1974. Simple models of diffusion and combined diffusion–infiltration metasomatism. In: *Geochemical Transport and Kinetics* (edited by Hoffman, A. W. *et al.*). Carnegie Institution of Washington, Washington D.C., 242–262.

Fyfe, W. S. 1976. Chemical aspects of rock deformation. *Phil. Trans. R. Soc. Lond.* **A283**, 221–228.

Ghent, E. D. & Stout, M. Z. 1981. Metamorphism at the base of the Semail ophiolite, southeastern Oman Mountains. *J. geophys. Res.* **86**, 2557–2572.

Jahns, R. H. 1967. Serpentinite of the Roxbury District, Vermont. In: *Ultramafic and Related Rocks* (edited by Wyllie, P. J.). Wiley, New York, 137–160.

Jamieson, R. A. & Strong, D. F. 1981. A metasomatic mylonite zone within the ophiolite aureole, St. Anthony complex, Newfoundland. *Am. J. Sci.* **281**, 264–281.

Kerrich, R., Fyfe, W. S., Gorman, B. E. & Allison, I. 1977. Local modification of rock chemistry by deformation. *Contr. Miner. Petrol.* **65**, 183–190.

Kirby, S. H. 1983. Rheology of lithosphere. *Rev. Geophys. Space Phys.* **21**, 1458–1487.

Kirby, S. H. 1985. Rock mechanics observations pertinent to the rheology of the continental lithosphere and the localization of strain along shear zones. *Tectonophysics* **119**, 1–27.

LaTour, T. E. & Kerrich, R. 1982. Microstructures, mineral chemistry and oxygen isotopes of two adjacent mylonite zones: A comparative study. In: *Issues in Rock Mechanics* (edited by Heuze, F. E. & Goodman, R. E.). *Proc. 23rd U.S. Symposium on Rock Mechanics*, 389–396.

Malpas, J. 1979. The dynamothermal aureole of the Bay of Islands ophiolite suite. *Can. J. Earth Sci.* **16**, 2086–2101.

Miller, R. B. 1980. Structure, petrology and emplacement of the ophiolitic Ingalls Complex, North-central Cascade Mountains, Washington. Unpublished Ph.D. thesis, University of Washington.

Miller, R. B. 1985. The ophiolitic Ingalls Complex, North-central Cascades, Washington. *Bull. geol. Soc. Am.* **96**, 27–42.

Miller, R. B. & Mogk, D. 1987. Ultramafic rocks of a fracture-zone ophiolite, North Cascades, Washington. *Tectonophysics* **142**, 261–289.

Misch, P. 1969. Paracrystalline microboudinage of zoned grains and other criteria for synkinematic growth of metamorphic minerals. *Am. J. Sci.* **267**, 43–63.

Misch, P. 1977. Bedrock geology of the North Cascades. In: *Geological Excursions in the Pacific Northwest* (edited by Brown, E. H. & Ellis, R. C.). Western Washington University, Bellingham, Washington, 1–62.

Murrell, S. A. F. 1985. Aspects of relationships between deformation and prograde metamorphism that cause evolution of water. In: *Advances in Physical Geochemistry, Vol. 4. Metamorphic Reactions: Kinetics, Textures and Deformation* (edited by Thompson, A. B. & Rubie, D. C.). Springer, Berlin, 211–241.

Nicolas, A., Boudier, F. & Bouchez, J. 1980. Interpretation of peridotite structures from ophiolitic and oceanic environments. *Am. J. Sci.* **280-A**, 192–210.

Nielsen, K. C. 1978. Tectonic setting of the northern Okanagan valley at Mara Lake, British Columbia. Unpublished Ph.D. thesis, University of British Columbia.

Raleigh, C. B. & Paterson, M. S. 1965. Experimental deformation of serpentinite and its tectonic implications. *J. geophys. Res.* **70**, 3965–3985.

Rohr, D. W. 1985. Fluid flow and alkali transport within a metamorphic terrane, western North Carolina. *Tectonophysics* **119**, 329–348.

Rumble, D., Ferry, J. M., Hoering, T. C. & Boucot, A. J. 1982. Fluid flow during metamorphism at the Beaver Brook fossil locality, New Hampshire. *Am. J. Sci.* **282**, 886–919.

Rutter, E. H. 1976. The kinetics of rock deformation by pressure solution. *Phil. Trans. R. Soc. Lond.* **A283**, 203–219.

Rutter, E. H., Peach, C. J., White, S. H. & Johnston, D. 1985. Experimental syntectonic hydration of basalt. *J. Struct. Geol.* **7**, 251–266.

Secor, D. T. 1965. Role of fluid pressure in jointing. *Am. J. Sci.* **263**, 633–646.

Sinha, A. K., Hewitt, D. A. & Rimstidt, J. D. 1986. Fluid interaction

and element mobility in the development of ultramylonites. *Geology* **14**, 883–886.

Snoke, A. W. & Calk, L. C. 1978. Jackstraw-textured talc-olivine rocks, Preston Peak area, Klamath Mountains, California. *Bull. geol. Soc. Am.* **89**, 223–230.

Trommsdorff, V. & Evans, B. W. 1974. Alpine metamorphism of peridotitic rocks. *Schweiz. miner. petrogr. Mitt.* **54**, 333–352.

Vance, J. A. & Dungan, M. A. 1977. Formation of peridotites by deserpentinization in the Darrington and Sultan areas. *Bull. geol. Soc. Am.* **88**, 1497–1508.

White, S. H., Burrows, S. E., Carreras, J., Shaw, N. D. & Humphreys, F. J. 1980. On mylonites in ductile shear zones. *J. Struct. Geol.* **2**, 175–187.

Williams, H. & Smyth, W. R. 1973. Metamorphic aureoles beneath ophiolite suites and alpine peridotites: tectonic implications with West Newfoundland examples. *Am. J. Sci.* **273**, 594–621.

Yardley, B. W. D. 1983. Quartz veins and devolatization during metamorphism. *J. geol. Soc. Lond.* **140**, 657–663.

Yardley, B. W. D. 1986. Fluid migration and veining in the Connemara Schists, Ireland. In: *Advances in Physical Geochemistry, Vol. 5. Fluid-rock Interactions During Metamorphism* (edited by Walther, J. V. & Wood, B. J.). Springer, Berlin, 109–131.

Zen, E-an. 1972. Gibbs free energy, enthalpy, and entropy of the rock-forming minerals: calculations, discrepancies, implications. *Am. Miner.* **57**, 524–553.